

Surface electronic structure of Tm(0001) and Yb(111)

M. Bodenbach, A. Höhr, C. Laubschat,* and G. Kaindl

Institut für Experimentalphysik, Freie Universität Berlin, Arnimallee 14, D-14195 Berlin-Dahlem, Germany

M. Methfessel

Institut für Halbleiterphysik, Walter-Korsing-Straße 2, D-15230 Frankfurt/Oder, Germany

(Received 14 June 1994)

Occupied *d*-like surface states were observed for the close-packed surfaces of Tm(0001) and Yb(111) metal films grown epitaxially on W(110) and Mo(110) substrates, respectively. In the case of Tm metal, the surface state exhibits almost no dispersion and is extended over the whole surface Brillouin zone, while in the case of Yb metal, it is restricted to a narrow region around the $\bar{\Gamma}$ point. The surface shifts of the *4f* binding energies on these close-packed surfaces were determined to be 0.47 ± 0.05 eV for Tm(0001) and 0.45 ± 0.03 eV for Yb(111). Both values are substantially smaller than reported previously for polycrystalline surfaces of the two metals. State-of-the-art band-structure calculations, based on density-functional theory, predict a flat surface state slightly *above* the Fermi energy. There is no obvious explanation for this inconsistency at the present time.

For quite some time, the surface electronic structure of rare-earth metals has been attracting a wide scope of experimental and theoretical efforts.¹ Most of the experimental work has been performed on polycrystalline materials, and has been devoted to an investigation of *4f* states. Since magnetic ordering of the Gd(0001) surface above the bulk Curie point of Gd metal was observed,² however, there has been growing interest in the surface valence-band electronic structure, requiring experiments on well-ordered monocrystalline surfaces. The preparation of clean surfaces of bulk single crystals of rare-earth metals is difficult, due to the large chemical reactivity of these metals, and does not seem to be a successful route.^{3,4} On the other hand, clean and well-ordered films of rare-earth metals can be grown epitaxially on W(110) and Mo(110) substrates.^{5–13} Recently, an intense surface state of *d* symmetry was observed for the Gd(0001) surface.¹⁰ This state is situated close to the Fermi level E_F , within a wide band gap around the $\bar{\Gamma}$ point of the surface Brillouin zone, exhibiting no dispersion. Spin-polarized photoemission experiments show that the photoelectrons emitted from this state are fully spin polarized in the ferromagnetic phase.¹¹ Band-structure calculations¹⁴ suggest that this state is derived from an unoccupied nonbonding bulk state of d_{z^2} symmetry, which is lowered in energy by a loss of kinetic energy in the vacuum region. These calculations, however, fail in predicting the correct magnetic¹¹ and structural¹⁵ properties of the Gd(0001) surface. In the meantime, a related surface state has been observed for the (0001) surface of Tb metal in its paramagnetic phase,⁴ and a direct relationship between the appearance of this surface state and the structural order at the surface has been established.¹³ Also, for La(0001), a partly occupied surface state was recently found by photoemission and inverse photoemission studies.¹⁶

In the present paper, we report on the observation of similar surface states for the elements at the end of the

rare-earth series, Tm and Yb. It is of particular interest that such a surface state has now also been observed for a divalent rare-earth metal, Yb. As in the case of Gd and Tb, the surface state appears for hcp Tm on the close-packed (0001) surface and is extended over nearly the whole surface Brillouin zone. For fcc Yb, the surface state also appears on the close-packed (111) surface, but is restricted to a narrow region around the $\bar{\Gamma}$ point. Scalar-relativistic calculations (which include all relativistic effects except spin-orbit coupling), based on the local-density approximation (LDA), predict a nondispersive surface state for Tm(0001). In contrast to the experimental result, however, the slab calculations predict this state to be unoccupied. For divalent Yb, no explicit surface state is predicted by theory, but the presence of bulk states just above the Fermi level allows for a surface resonance. Apart from the surface state, surface shifts of the *4f* binding energies to higher values by $\delta_s = 0.47 \pm 0.05$ and 0.45 ± 0.03 eV were determined for Tm(0001) and Yb(111), respectively. For Yb metal, this value is in good agreement with a literature value,¹⁷ while for Tm metal the shift is considerably smaller than reported previously for polycrystalline samples^{18,19} and obtained theoretically by LDA-slab calculations.²⁰

The photoemission (PE) experiments were performed with a rotatable hemispherical electron energy analyzer (Vacuum Science Workshop, ARIES) using synchrotron radiation from the TGM1 and TGM4 beamlines of the Berliner Elektronenspeicherring für Synchrotronstrahlung, BESSY. Monocrystalline films of Tm and Yb metal were prepared by thermal evaporation of the pure rare-earth metals from resistively heated tungsten coils onto clean W(110) and Mo(110) substrates, respectively. Film thicknesses were measured by means of a quartz microbalance and adjusted to about 100 Å. The evaporation rates were about 5 Å/min, and the pressure in the experimental chamber (with a base pressure of 5×10^{-11} mbar) rose briefly to 5×10^{-10} mbar during deposition.

The as-grown films revealed sharp low-energy electron-diffraction (LEED) patterns. Contaminations were checked by Auger spectroscopy and via the O 2*p* PE signal. In case of Tm, small oxygen contaminations could be detected corresponding to $\cong 0.02$ monolayers.

Scalar-relativistic nonmagnetic band-structure calculations were performed using the full-potential linear muffin-tin orbital (FP-LMTO) method as described in Refs. 21 and 22, with some modifications needed for an accurate description of the surface.²³ The method was applied to seven-layer slabs, separated by approximately ten layers of vacuum. The *k*-space integration was done with a mesh of 19 irreducible points. Since the LDA cannot describe the correlation between *f* states properly, these were treated as core states with a fixed occupation of $4f^{12}$ for Tm and $4f^{14}$ for Yb. The ideal truncated bulk geometry at the experimental lattice constant was used; it was also tested that possible surface relaxations would not affect the conclusions. For the bulk bands, the calculated energy dispersion curves are in very good agreement with previous band-structure calculations for Tm (Ref. 24) and Yb (Refs. 25 and 26) metal. The calculations also provide values for the surface core-level shifts and the work functions of the metal surfaces. In view of the discrepancy between theory and experiment, we emphasize that the calculational method used has been shown to be of high accuracy and reliability in the context of the transition-metal surfaces.²³ Further technical details are described in the reference.

Figure 1 displays angle-resolved PE spectra in the valence-band region of Tm(0001), taken with the sample at room temperature at normal emission and for two different photon energies. The spectral features in the binding-energy (BE) region from 4 to 11 eV represent PE from the open Tm(III)- $4f^{12}$ shell and can be described by a superposition of two $4f^{11}$ final-state multiplets,²⁷ which are separated by 0.47 ± 0.05 eV from each other and reflect signals from bulk (solid subspectrum) and surface atoms (dashed subspectrum), respectively. It should be noted that the agreement between theoretical intensities of the individual multiplet lines (taken from Ref. 27 and the experimental values) is relatively poor, and the relative intensities of several lines had to be varied from the theoretical values in order to obtain a reasonable description of the spectra. We found that the relative line intensities are strongly photon energy dependent, which can be attributed to cross-section effects and/or photoelectron diffraction within the ordered layer. The multiplet splittings had to be stretched by a factor of 1.10 as compared to the values given in Ref. 27.

The observed surface shift is considerably smaller than the previously reported experimental value of 0.70 ± 0.05 eV, which had been measured for polycrystalline Tm metal films,^{18,19} and the theoretical value of 0.63 eV calculated by the LDA-slab method for the close-packed Tm(0001) surface.²⁰ The discrepancy with the previously reported surface shift for Tm metal can be explained by a relatively rough surface in case of a polycrystalline sample, i.e., by the presence of atomic surface sites with different and also lower coordinations. This will lead to a broadening and a shift to higher BE of the surface PE component as

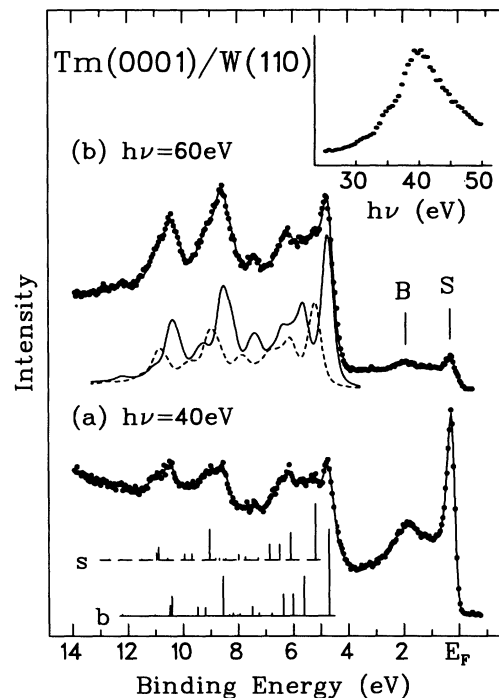


FIG. 1. Angle-resolved photoemission (PE) spectra of Tm(0001) taken at normal emission for two different photon energies. The inset shows the variation of the intensity of the PE peak *S* as a function of photon energy, derived from a constant-initial-state measurement after normalization to equal photon flux.

compared to the situation of a well-ordered and smooth close-packed surface layer.^{13,17} On the other hand, the observed surface core-level shift for Tm(0001) is larger than the recently reported values for Tb(0001), $\delta_s = 0.26 \pm 0.03$,¹³ and Gd(0001), $\delta_s = 0.29 \pm 0.03$.²⁸ This is most probably due to a systematic increase of the surface core-level shifts with atomic number across the series of rare-earth metals.¹⁸ The present calculations give a surface shift of 0.60 eV, which is in good agreement with the previous LDA result. This value describes a pure initial-state property and should not be compared directly with the experimentally derived shift. Recent calculations of final-state screening effects for the $4d$ -transition metals have shown that, at the beginning of the series, final-state screening is more effective at the surface than in the bulk, leading to a reduction of the expected surface core-level shifts by 0.12 and 0.16 eV for the close-packed surfaces of Y and Mo metal, respectively.²⁹ Assuming a similar behavior for the $5d$ -transition element Tm, the calculated initial-state shift is in good agreement with the experimental result. We note here that a separation of initial- and final-state contributions to δ_s has recently been achieved for Gd(0001), supporting this view.²⁸

The valence-band emission consists of two peaks *S* and *B*, at binding energies of $\cong 0.2$ and $\cong 1.7$ eV, respectively. As is evident from the photon-energy dependencies of the photoemission cross sections of these states, both states

contain practically no $4f$ symmetry, as one might speculate in analogy to the well-known Kondo peak in Ce systems.³⁰ The inset in Fig. 1 shows the variation in the intensity of the PE peak S as a function of photon energy, derived from a constant-initial-state (CIS) PE measurement with proper normalization to equal photon flux. This curve shows that the PE cross section of the surface state S peaks at a photon energy of ≈ 40 eV. A similar behavior is known for the PE signals from d states of several rare-earth metals^{31,32} and also from Ca metal,³³ having been attributed to $p \rightarrow d$ Fano resonances in the neighborhood of the $5p$ and $3p$ thresholds, respectively. The photon-energy-dependent intensity variations of peak B are similar to those of peak S . On the basis of these observations, we assign d symmetry to both peaks S and B . In analogy to the valence-band PE spectrum of Gd(0001), which contains very similar structures,¹⁰ peak B is assigned to emission from the Δ_2 band, while peak S is assigned to a surface state situated in a broad gap of the surface-projected bulk band structure.^{14,24} In fact, peak S can be quenched by exposure to 1 ML of oxygen (spectrum not shown here), confirming the surface-related nature of this state.

The angular dependence of the valence-band PE peaks recorded in the $\bar{\Gamma}\bar{M}\bar{\Gamma}$ direction is shown in Fig. 2, where the \bar{M} point would correspond to an angle of $\theta = 16.6^\circ$. Peak B reveals a strong dispersion with θ (and k), in agreement with its assignment as a direct-transition feature from the bulk Δ_2 band. For the position of the critical point Γ_4^+ , an energy of 2.3 eV is predicted from the present band-structure calculation, in agreement with previous results.²⁴ This value is somewhat larger than the value of 1.8 eV observed in the present experiment. The same discrepancy between theory and experiment was also observed for Gd metal, where the respective energy positions are almost identical to those obtained here for Tm metal.^{10,11,14} We conclude from the large surface-to-bulk intensity ratio observed for the $4f$ states, however, that contributions to peak B stem almost completely from the first two atomic layers and are not necessarily characteristic of the real bulk. This might be an explanation for the observed discrepancy between experi-

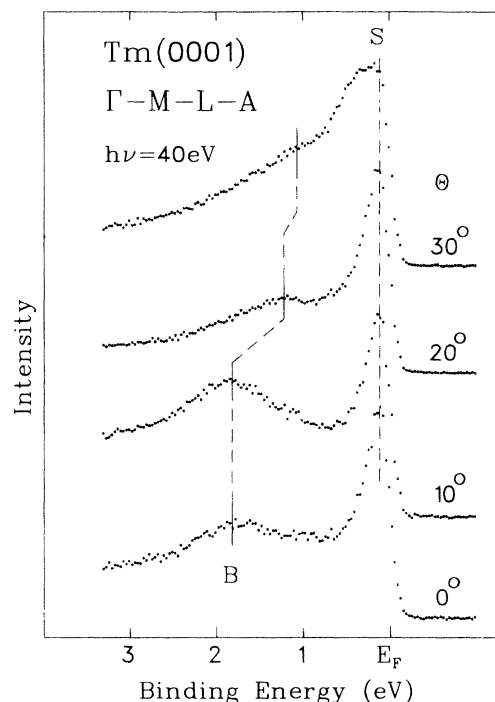


FIG. 2. Angular dependence of the Tm(0001) valence-band PE spectrum taken in the $\bar{\Gamma}\bar{M}\bar{\Gamma}$ direction with 40-eV photons.

ment and theory, as will be discussed below.

Peak S shows almost no dispersion. A corresponding nondispersive surface state is also found in the present slab calculations, situated around the $\bar{\Gamma}$ point as shown in Fig. 3(a). In contrast to the experimental result, however, this state is found to be unoccupied. The situation is not significantly changed by modifications such as inward or outward surface relaxation by any reasonable amount. A similar state had also been found recently in a slab calculation for the (0001) surface of Gd metal in its ferromagnetic phase.¹⁴ There, the surface state is widely split by magnetic exchange interaction, and the minority-spin component is found to be occupied, a prediction that is in

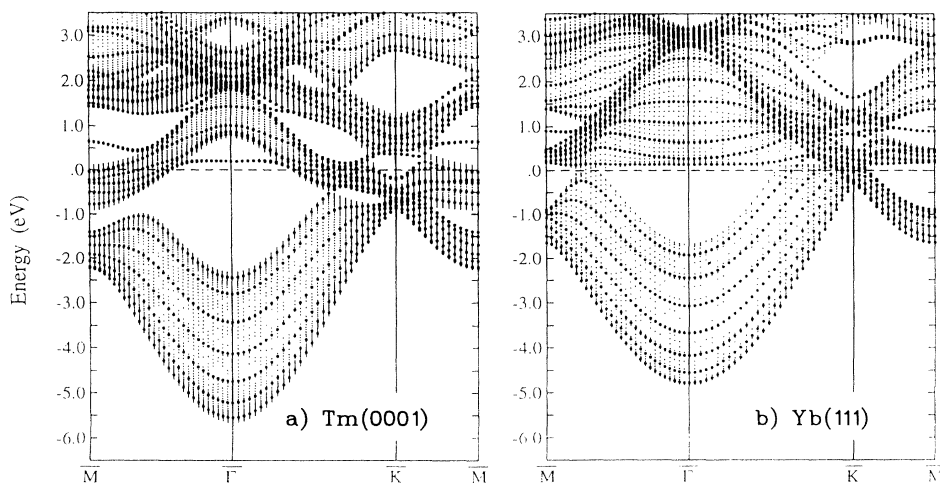


FIG. 3. Calculated band structure in the surface Brillouin zone of a seven-layer slab (large dots) superimposed on the projected bulk bands (shaded) for (a) Tm(0001) and (b) Yb(111). A surface state can be identified where a slab state falls into an unoccupied pocket of the projected bulk bands.

conflict with experimental results.^{11,34} In the present case of Tm, the slab calculation results in a nonsplit surface state, since the system is in its paramagnetic phase and spin-orbit interaction was not taken into account. For La(0001), a surface state both below and above E_F could recently be identified by PE and inverse PE experiments;¹⁶ a similar situation has also been found for Gd(0001).^{10,34} This suggests that also in Tm metal the surface state is only partly filled. On the other hand, such a weakly dispersive state corresponds to a large density of states, and—by reason of charge neutrality—the occupancy of this state has to be coupled to a depopulation of other states and an energy relaxation of the whole valence-band structure at the surface. In a simple rigid-band model this would lead to a shift of the occupied bands toward the Fermi energy, which in fact could explain the mentioned discrepancy between theoretical prediction and experimental observation of the energy of the Γ_4^+ point. Without having additional data, we tend to believe that the missing spin-orbit coupling cannot explain such major changes of the surface band structure. Thus we have to conclude that our careful measurements and calculations presently do not lead to a fully consistent picture of the surface electronic structure of Tm(0001).

In addition to Tm(0001), we have also studied the close-packed (111) surface of fcc Yb metal, which corresponds to the (0001) surface in hcp stacking. Figure 4 shows valence-band PE spectra of Yb(111), taken in nor-

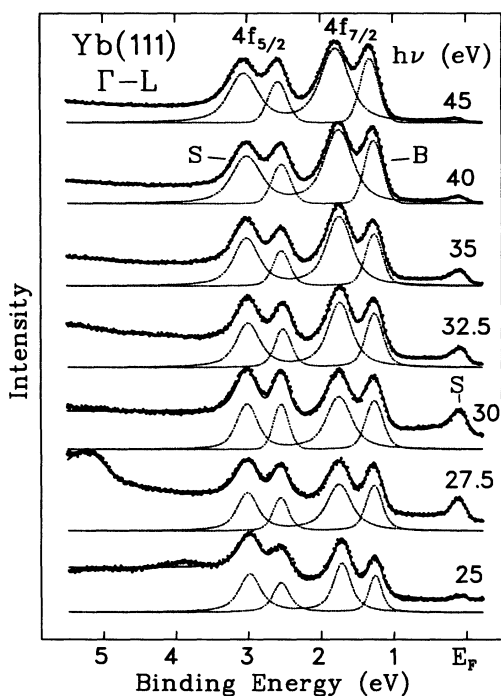


FIG. 4. Valence-band PE spectra of Yb(111) taken in normal-emission geometry for various photon energies. The additional feature in the $h\nu=25$ - and 27.5 -eV spectra at binding energies of 3.9 and 5.0 eV, respectively, are caused by an $O_{II,III}VV$ Auger transition.

mal emission for various photon energies. Figure 3(b) gives the results of the present slab calculations for the electronic structure of Yb metal, projected onto the (111) surface Brillouin zone. The dominant structure in the PE spectra in the BE region from 1 to 3 eV corresponds to emission from the filled $4f$ shell of Yb(II), consisting of two spin-orbit-split doublets, which are separated from each other by a surface core-level shift of $\delta_s = 0.45 \pm 0.03$ eV. The magnitude of this shift agrees well with previous results for close-packed Yb surfaces,^{17,33} and is again strikingly smaller than the values around 0.6 eV obtained for polycrystalline surfaces.¹⁸ Note that δ_s for Yb(111) is very close to δ_s for Tm(0001). We add, however, that both the initial and final states of these metals are different, and the similarity of the two shifts is therefore accidental. The position of the bulk component, the spin-orbit splitting, and the intensity ratio of the $4f_{7/2}$ and $4f_{5/2}$ components are in full agreement with the literature.¹⁷ The slab calculations give an initial-state surface core-level shift of 0.33 eV, which in contrast to the case of Tm metal is smaller than the experimental value. In Yb metal, the s bands are almost filled, while the d states are almost empty. This situation is in some way analogous to the one at the end of the $4d$ series, where the d states become filled and the s band is empty. There final-state screening leads to an increase of the surface core-level shift, and the same mechanism may be responsible for the larger experimental value of the surface core-level shift observed for Yb metal.

The most exciting feature in the spectra of Fig. 4, however, is the sharp structure S close to E_F , displaying a strong photon-energy dependence of its intensity with a maximum around 30 eV and disappearing for photon energies above 40 eV. This energy dependence of the PE cross section is probably the reason why this structure had not been observed in previous work on single-crystalline Yb(111) surfaces.³⁵ The photon-energy dependence of this peak is very similar to that of the surface state on Tm(111); only the maximum is shifted by ≈ 10 eV to lower energies. As in the case of Tm, this state exists in a broad energy gap around the $\bar{\Gamma}$ point of the surface-projected bulk band structure [see Fig. 3(b)], suggesting again an assignment of this peak to a d -like surface state. Unfortunately, quenching of this state by oxygen exposure did not work satisfactorily, with the state remaining stable even for coverages exceeding 1 L. Thus it cannot be fully ruled out that this state represents a bulk PE feature of Yb metal. On the other hand, it has been pointed out that a shift of the unoccupied $5d$ states by 0.1 Ry to higher energies would cause the formation of a p -like electron pocket around the L point of the bulk band structure,²⁵ which might be responsible for the observed peak close to the Fermi level. From a comparison of the calculated band structure with the measured unoccupied density of states,³⁵ however, there is no hint of such a shift of the d band. Moreover, interpreting the Fermi level peak as a bulk feature and using a free-electron parabola fitted to the s band for the final states, the large emission observed for photon energies of 27.5 and 30 eV would correspond to wave vectors close to the Γ point, in contrast to theoretical prediction. From the

visibility of this state over a relatively large photon-energy range, one would further conclude that this non-dispersive state is extended in the ΓL direction over the whole bulk Brillouin zone, which is in contrast to the calculated dispersive behavior of the conduction-band states. Thus an origin of this peak from the bulk band structure seems unlikely.

Figure 5 shows the angular dependence of the Fermi-level peak S , measured for a photon energy of 30 eV in the $\bar{\Gamma M}$ direction. For this photon energy, the \bar{M} point would correspond to an angle of $\Theta \cong 18.0^\circ$. In contrast to the behavior of the surface state on Tm(0001), the Fermi-level peak disappears for angles larger than about 5° . This critical angular dependence can be a further reason why this state has never been observed before. The difference in the behavior with respect to Tm can be understood qualitatively within a simple rigid-band model. Here, when going from trivalent Tm to divalent Yb, the Fermi level is lowered and only the lowest-lying parts of the surface band remain occupied. The slab calculation, however, does not reveal an explicit surface state for Yb(111) [see Fig. 3(b)]. At best, a surface resonance can be expected above, but close to the Fermi level.

In summary, both trivalent Tm metal and divalent Yb metal have occupied surface states on their close-packed surfaces. In the case of Yb(111), this state is restricted to a narrow zone around the $\bar{\Gamma}$ point, which is in contrast to the situation in the trivalent rare-earth metals, where the surface state extends over almost the whole surface Brillouin zone. *Ab initio* calculations for the two surfaces studied predict a surface state or resonance of d character near the Fermi energy, but these states lie above the Fermi energy and are unoccupied. Further work is needed to determine the reason for this discrepancy. The surface core-level shifts of the $4f$ states are found to be equal within the error bars for the two close-packed metal sur-

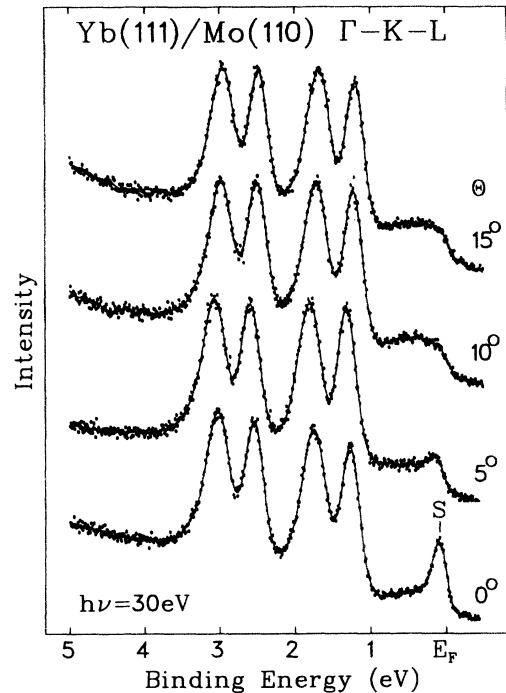


FIG. 5. Angular dependence of the valence-band PE spectrum of Yb(111), taken with 30-eV photons in the $\bar{\Gamma M}$ direction.

faces, amounting to $\delta_s = 0.47 \pm 0.05$ and 0.45 ± 0.05 eV for Tm(0001) and Yb(111), respectively.

This work was supported by the Bundesminister für Forschung und Technologie, Project No. 05-5KEAXI-3/TP01, and the Deutsche Forschungsgemeinschaft, Sonderforschungsbereich-290, TPA06.

*Permanent address: Institut für Oberflächen- und Mikrostrukturphysik, Technische Universität Dresden, Mommsenstraße 13, D-01062, Dresden, Germany.

¹For a general overview, the reader is referred to the series *Handbook on the Physics and Chemistry of Rare Earths*, edited by K. Gschneidner (North-Holland, Amsterdam, 1993).

²C. Rau and S. Eichner, Phys. Rev. B **34**, 6347 (1986).

³S. D. Barrett, Surf. Sci. Rep. **4**, 271 (1992).

⁴S. C. Wu, H. Li, Y. S. Li, D. Tian, J. Quinn, F. Jona, D. Fort, and N. E. Christensen, Phys. Rev. B **45**, 8867 (1992).

⁵A. Kolaczkiwicz and E. Bauer, Surf. Sci. **175**, 487 (1986).

⁶D. Weller, S. F. Alvarado, W. Gudat, K. Schröder, and M. Campagna, Phys. Rev. Lett. **54**, 1555 (1985); J. Appl. Phys. **59**, 2908 (1986).

⁷A. Stenborg and E. Bauer, Phys. Rev. B **36**, 5840 (1987).

⁸A. Stenborg, J. N. Anderson, O. Bjorneholm, A. Nilson, and N. Mårtensson, Phys. Rev. Lett. **63**, 187 (1989).

⁹U. Stetter, M. Farle, K. Baberschke, and W. G. Clark, Phys. Rev. B **45**, 503 (1992).

¹⁰B. Kim, A. B. Andrews, J. L. Erskin, K. J. Kim, and B. N. Harmon, Phys. Rev. Lett. **68**, 1931 (1992).

¹¹G. A. Mulhollan, K. Garrison, and J. L. Erskin, Phys. Rev.

Let. **69**, 3240 (1992).

¹²K. Starke, E. Navas, L. Baumgarten, and G. Kaindl, Phys. Rev. B **48**, 1329 (1993).

¹³E. Navas, K. Starke, C. Laubschat, E. Weschke, and G. Kaindl, Phys. Rev. B **48**, 14 753 (1993).

¹⁴R. Wu, C. Li, A. J. Freeman, and C. L. Fu, Phys. Rev. B **44**, 9400 (1991).

¹⁵J. Quinn, Y. S. Li, F. Jona, and D. Fort, Phys. Rev. B **46**, 9694 (1992).

¹⁶A. Fedorov, A. Höhr, E. Weschke, K. Starke, V. K. Adamchuk, and G. Kaindl, Phys. Rev. B **49**, 5117 (1994).

¹⁷W. D. Schneider, C. Laubschat, and B. Reihl, Phys. Rev. B **27**, 6538 (1983).

¹⁸F. Gerken, A. S. Flodström, J. Barth, L. I. Johansson, and C. Kunz, Phys. Scr. **32**, 43 (1985).

¹⁹M. Domke, C. Laubschat, M. Prietsch, T. Mandel, G. Kaindl, and W. D. Schneider, Phys. Rev. Lett. **56**, 1287 (1986).

²⁰A. M. Begley, R. G. Jordan, W. M. Temmermann, and P. I. Durham, Phys. Rev. B **41**, 11 780 (1990).

²¹M. Methfessel, Phys. Rev. B **38**, 1537 (1988).

²²M. Methfessel, C. O. Rodriguez, and O. K. Anderson, Phys. Rev. B **40**, 2009 (1989).

- ²³M. Methfessel, D. Hennig, and M. Scheffler, *Phys. Rev. B* **46**, 4616 (1992).
- ²⁴P. Strange, W. M. Fairbairn, and P. M. Lee, *J. Phys. F* **13**, 649 (1983).
- ²⁵G. Johansen and A. R. Mackintosh, *Solid State Commun.* **8**, 121 (1970).
- ²⁶Y. Kubo, *J. Phys. F* **17**, 383 (1987).
- ²⁷F. Gerken, *J. Phys. F* **13**, 703 (1983).
- ²⁸A. V. Fedorov, E. Arenholz, K. Starke, E. Navas, L. Baumgarten, C. Laubschat, and G. Kaindl, *Phys. Rev. Lett.* **73**, 601 (1994).
- ²⁹M. Methfessel, D. Hennig, and M. Scheffler (unpublished).
- ³⁰E. Weschke, C. Laubschat, C. T. Simmons, M. Domke, O. Strebel, and G. Kaindl, *Phys. Rev. B* **44**, 8304 (1991).
- ³¹V. Murgai and Y. S. Huang, *Solid State Commun.* **66**, 329 (1988).
- ³²D. J. Friedman, C. Carbone, K. A. Bertness, and I. Lindau, *J. Electron. Spectrosc. Relat. Phenom.* **41**, 59 (1986).
- ³³J. Barth, I. Chorkendorff, F. Gerken, C. Kunz, R. Nyholm, J. Schmidt-May, and G. Wendin, *Phys. Rev. B* **30**, 6251 (1984).
- ³⁴A. V. Fedorov, K. Starke, and G. Kaindl, *Phys. Rev. B* **50**, 2739 (1994).
- ³⁵A. Nilsson, A. Stenborg, O. Björneholm, N. Mårtensson, J. N. Andersen, and C. Wigren (unpublished).
- ³⁶J. K. Lang, Y. Baer, and R. A. Cox, *J. Phys. F* **11**, 121 (1981).

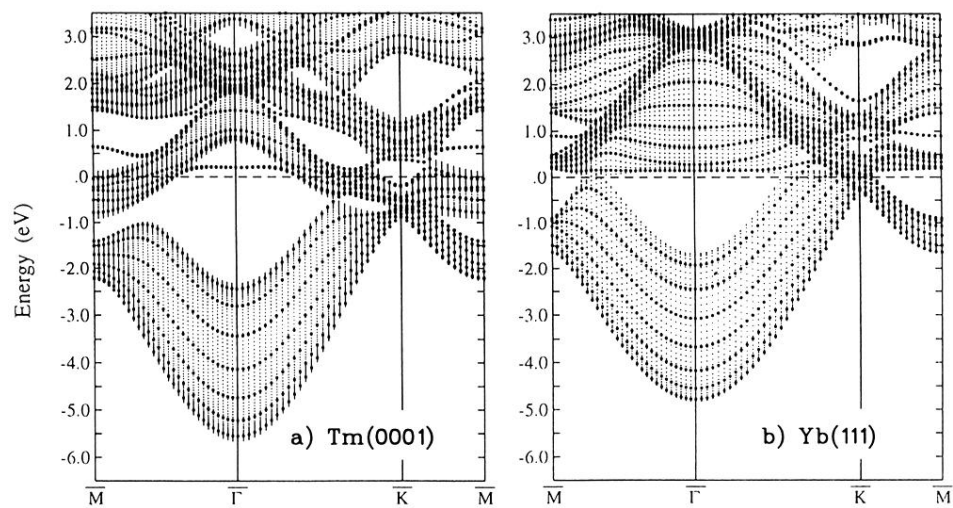


FIG. 3. Calculated band structure in the surface Brillouin zone of a seven-layer slab (large dots) superimposed on the projected bulk bands (shaded) for (a) Tm(0001) and (b) Yb(111). A surface state can be identified where a slab state falls into an unoccupied pocket of the projected bulk bands.